Drug Development and Industrial Pharmacy, 25(8), 885–895 (1999)

RESEARCH PAPER

Compaction Properties of Powders: The Relationship Between Compression Cycle Hysteresis Areas and Maximally Applied Punch Pressures

Davar Khossravi*

DuPont Merck, Pharmaceutical Research and Development, Experimental Station, PO Box 80400, Wilmington, DE 19880

ABSTRACT

The consolidation behaviors of various pharmaceutical solids were characterized by investigating the relationship between the calculated hysteresis areas and the maximally applied punch pressures. An Instron universal testing apparatus and an instrumented die were used to generate compression cycle profiles at various maximally applied punch pressures for the materials studied. Based on the profiles obtained, hysteresis areas were calculated for the materials studied as a function of maximally applied punch pressures. Furthermore, model profiles describing the plastic and brittle fracture processes were utilized to derive mathematical relationships between the calculated hysteresis cycle areas and the maximally applied punch pressures. The mathematical relationships derived indicate that a linear relationship between hysteresis areas and maximally applied punch pressures exists for plastic materials, whereas for brittle materials the hysteresis areas are related to the square of the maximally applied punch pressures. Experimental data obtained support the mathematical relationships derived. The goodness of fit to the models derived is used to rank order the consolidation mechanism of various drugs and pharmaceutical excipients.

* Present address: 3M Pharmaceuticals, 3M Center, Building 260-4N-12, St. Paul, MN 55144-1000. E-mail: dkhossravi@mmm.com

INTRODUCTION

Hysteresis areas as a function of maximally applied punch pressures have been used to elucidate the mechanism of powder consolidation into a tablet body (1,2). The primary interest in identifying the mechanism of powder consolidation lies in the characterization of the pharmaceutical excipient and/or the drug compound used in solid dosage form formulations (3–8). It is anticipated that such information would aid in further understanding of the final tablet quality in terms of the quality of bonds formed within the tablet matrix and alleviation of capping or chipping problems associated with the tableting operation (9–11).

The two primary consolidation mechanisms in pharmaceutical powders are plastic deformation and brittle fracture. The plastic deformation process entails the deformation of individual particles under high pressure, with the subsequent flow and creep of the material under pressure to form a solid compact. In the brittle fraction process, the individual particles fracture into smaller particles under the applied pressure. Subsequently, these smaller particles form a compact at the higher applied pressures and smaller volumes within which the material is confined. These two basic consolidation mechanisms are present to a varying extent in different materials. Other deformation mechanisms, such as elastic and viscoelastic deformation, may also be present; however, they do not contribute significantly to the consolidation of the compact and the subsequent tablet bond formation.

Various experimental methods have been used to distinguish between the plastic deformation and brittle fracture mechanisms of powder consolidation; the use of compression cycle profiles is one such method (1–3, 12,13). Compression cycle profiles characterize the extent of pressure distribution within the powder bed, as well as in the formed tablet matrix. Based on these profiles, loading and unloading slopes, as well hysteresis areas, can be calculated.

The current paper focuses on the calculated hysteresis areas as a function of maximally applied punch pressures. Previously, mathematical relationships have been derived that indicate that, for plastic materials, a linear relationship between hysteresis areas and maximally applied upper-punch pressure exists, whereas for brittle materials, a quadratic relationship is expected (1). A limited experimental test (2) of the mathematical model utilizing plastic materials such as polyvinyl alcohol, polyvinyl chloride, and a copolymer of the two could not establish such a relationship, casting doubts as to the validity of the underlying assumptions used to derive the relationship (1).

The present paper investigates a comprehensive number of pharmaceutical excipients in order to explore the existence of such a relationship. Furthermore, more realistic model compression cycle profiles based on the compression cycle profiles obtained are utilized to derive the mathematical relationship between the calculated hysteresis areas and the maximally applied punch pressure for plastic and brittle fracture materials. A novel multicompression cycle is used to investigate the hysteresis areas for the first compression cycle, which is associated with the powder bed, and the fifth compression cycle, which is associated with the property of the formed tablet body.

EXPERIMENTAL

The pharmaceutical active ingredients and excipients were acetaminophen USP; anhydrous lactose NF; aspirin USP; Avicel microcrystalline cellulose, NF type PH-112; Avicel microcrystalline cellulose, NF type PH-102; Carbowax Sentry polyethylene 1450 flake NF; Carbowax Sentry polyethylene 8000 powder NF; cornstarch NF; high-density polyethylene; Klucel HXFNF; Klucel HXF; lactose hydrous NF; Sentry Polyox WSRN-750 NF; Sentry Polyox WSRN-303 NF; sodium chloride AR crystals ACS; sodium citrate anhydrous powder USP; and sucrose NF. The lot numbers and manufacturers of these materials are described in an earlier paper (3); all the materials were stored at 68°F–72°F and 40–50% relative humidity (RH).

The compression cycle profiles were generated using an Instron (model 5567, Canton, MA) with a load cell of 30 kN and an especially fabricated instrumented die that was calibrated. The specific methodology of the fabrication (14) and calibration of the instrumented die have been presented previously (3). Merlin software was used to control the Instron; specifically, the crosshead was programmed to move down at a rate of 5 mm/min until a pressure of 74, 148, or 223 MPa was reached. Once the programmed pressure was achieved, the Instron was instructed to move up at the same rate until a force of nearly zero was measured (0.02 kN). The software was programmed to repeat this cycle immediately four more times. The software was also programmed to collect data points each time the applied pressure changed by 0.14 MPa. The data points consisted of the applied load, transmitted load, and crosshead distance traveled, and they

were collected as a function of time. The applied load and transmitted load were then used to calculate the applied pressure and the transmitted pressure to construct the compression cycle profiles. The trapezoidal rule was used to calculate the hysteresis area for the compression cycle profiles obtained.

The compression cycle profile for each of the materials listed was generated three separate times, one corresponding to each maximum applied pressure listed. After each profile was generated, the compact was discarded, and fresh materials were used in order to generate the compression cycle profile of the material at a different maximally applied pressure. An appropriate amount of material was placed into the die to ensure coverage of the sensing element. The die was also lightly coated with magnesium stearate prior to addition of the materials to aid in lubrication.

RESULTS AND DISCUSSION

The compression cycle profiles obtained for polyethylene glycol 1450 are presented in Fig. 1. The three compression cycle profiles presented represent the material being compressed to various maximum applied punch pressures (74, 148, and 223 MPa). Polyethylene glycol is a soft, low molecular weight polymeric material that is known to consolidate by plastic deformation (3,13). The loading portions of the profiles obtained indicate that there is a negligible constant amount of yield in all the profiles, followed by a linear rise. The unloading portions indicates that there is a relatively constant amount of lag (yield) between the maximum applied pressure and the pressure at which the transmitted pressure begins to fall in a linear fashion with the applied pressure. For all three compression cycles presented, there are no residual die wall pressures present, with the profiles returning to the point of origin. The compression cycle profiles as a function of applied pressure for the fifth compression cycle are practically superimposable on the compression cycle profiles presented for the first compression cycle. This indicates that the yield process that occurs during the tableting of this material is similar in the first cycle, as well as each subsequent cycle, which has been discussed previously (3).

The compression cycle profiles obtained for sodium citrate appear in Fig. 2. Sodium citrate is known to undergo consolidation by brittle fracture (5). The loading portions of the profiles indicate that initially there is a constant amount of yield, followed by a linear rise until the maximum applied punch pressure is reached. The unloading portions of the profiles indicate that there is a linear profile associated with the unloading portion, with a minor curvature as the applied pressure reaches zero. However, the amount of residual die wall pressure on the die is dependent on the maximum amount of applied

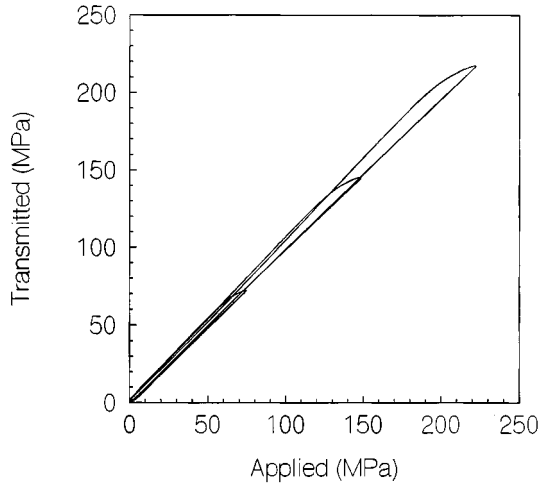

Figure 1. Compression cycle profiles for polyethylene glycol 1450. The profiles correspond to maximally applied pressures of 74, 148, and 223 MPa. The profiles are for the first compression cycle; subsequent compression cycles are superimposable on the first compression cycle profiles.

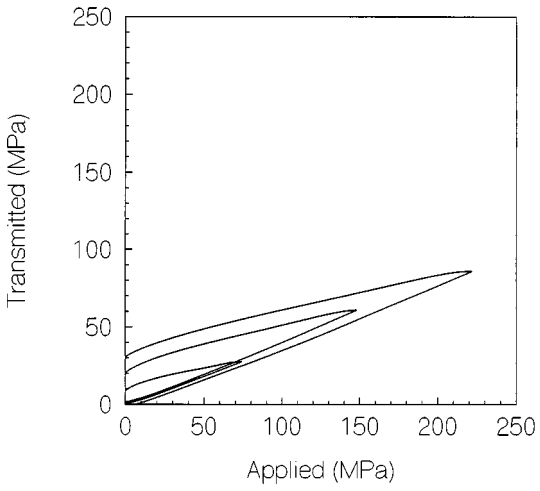

Figure 2. Compression cycle profiles for sodium citrate corresponding to the maximally applied pressures of 74, 148, and 223 MPa. The profiles are for the first compression cycle.

pressure. The compression cycle profiles for sodium citrate as a function of applied pressure for the fifth compression cycle appear in Fig. 3. The loading portions of these profiles originate at the residual die wall pressure associated with the first compression cycle and are extremely linear. The unloading profiles are also linear, with minor curvature associated at both ends. These profiles represent the elastic deformation of the material, which is similar in nature to the plastic model with the exception that the point of origin has been shifted to represent the residual die wall pressure.

The calculated hysteresis areas and the residual die wall pressures for all the compounds studied as a function of maximally applied punch pressures are reported in Table 1. The reported residual die wall pressures are the actual die wall pressure measurements when the corresponding applied punch pressure is zero. A plot of the calculated hysteresis areas as a function of compression cycle number indicates that, by the fifth compression cycle, steady state has been established (Fig. 4). For a plastic material such as polyethylene glycol 1450, there is no drastic difference between the initial and the subsequent compression cycles. For brittle fracture materials such as sucrose and sodium citrate, there is a drastic decline in the calculated hysteresis areas that is evident on the second compression cycle. This decline plateaus on subsequent compression cycles and is most drastic for sodium chloride.

A plot of the hysteresis areas for the first compression cycle as a function of the maximum applied pressure for plastic materials such as PEG 1450, Klucel HXFNF, and Myplx indicates an approximately linear relationship between the calculated hysteresis area and the maximally applied pressure (Fig. 5). For brittle materials, a linear relationship is not observed as a function of the maximum applied pressure. However, a plot of the hysteresis areas as a function of the maximum applied pressure squared is linear for brittle materials such as anhydrous lactose, sucrose, and sodium citrate (Fig. 6). These observations are consistent with the derivations of Carstensen and Toure (1), which claim that, for plastic materials, there is a linear relationship with the maximum applied pressure, whereas for brittle materials, the relationship is second order with respect to the maximum pressure applied. In their work, Carstensen and Toure utilized a hypothetical model for the plastic and brittle material in order to derive equations relating the hysteresis areas as a function of maximally applied punch pressures. In the present derivation, models based on the actual profiles measured are used to derive mathematical relationships between the hysteresis areas and the maximally applied punch pressures.

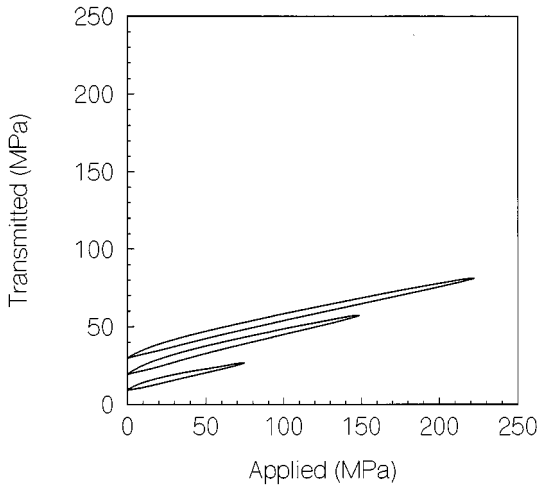

Figure 3. Compression cycle profiles for sodium citrate corresponding to the maximally applied pressures of 74, 148, and 223 MPa. The profiles are for the fifth compression cycle.

Derivation of Mathematical Relationships Between Hysteresis Areas and the Maximally Applied Punch Pressures

Plastic Materials

Based on the compression cycle profiles obtained, a relationship between the calculated hysteresis areas and the maximally applied punch pressures can be derived. To simplify the derivation of such equations, a simplified compression cycle profile is utilized. For plastic materials, this profile is depicted in Fig. 7. In this figure, L denotes the loading slope, U denotes the unloading slope, M denotes the maximum applied punch pressure, and Y denotes the yield point at which the relatively flat portion of the unloading slope ceases and the linear unloading slope describes the unloading event. It is assumed that the quantity Y, which is the yield pressure of the material, is constant. The hysteresis area for a material exhibiting a plastic profile can then be calculated by the following equation:

$$\text{Hysteresis area} = \int_0^{M-Y} Up\,dp + \int_{M-Y}^{M} U(M - Y)dp - \int_Y^M (Lp - LY)dp \quad (1)$$

Table 1

Residual Die Wall Pressure Remaining on the Die After the First and Fifth Compression Cycles and the Calculated Hysteresis Areas for All Five Cycles

	Maximum Applied Pressure (MPa)	Residual Die Wall Pressure (MPa)		Calculated Hysteresis Area (MPa^2)					Percentage Change
		Cycle 1	Cycle 5	Cycle 1	Cycle 2	Cycle 3	Cycle 4	Cycle 5	
Acetaminophen	223	14.8	15.1	6290	3579	3027	2813	2720	43
	148	12.4	13.4	2500	1437	1194	1095	1055	42
	74	6.6	7.2	636	371	331	311	298	47
Anhydrous lactose	223	44.8	44.6	7283	1772	1449	1346	1285	18
	148	26.2	27.2	2862	909	765	714	679	24
	74	11.1	11.2	599	230	212	203	201	34
Aspirin	223	7.1	11.0	4300	3584	3442	3383	3357	78
	148	4.5	6.7	1564	1332	1299	1280	1275	82
	74	4.0	4.7	526	423	409	402	395	75
Avicel PH102	223	9.7	11.9	4860	3160	2767	2558	2434	50
	148	10.3	11.9	2217	1452	1276	1203	1155	52
	74	7.6	8.1	585	326	296	283	274	47
Avicel PH112	223	9.0	10.5	4914	3197	2834	2663	2555	52
	148	9.7	10.3	2151	1293	1132	1054	1010	47
	74	7.1	7.9	585	334	302	287	276	47
Avicel PH302	223	14.0	14.0	5666	3266	2882	2689	2581	46
	148	13.4	15.0	2599	1421	1230	1139	1090	42
	74	8.2	8.7	590	310	277	263	254	43
Cornstarch	223	3.1	6.4	4942	4093	3753	3539	3383	68
	148	5.6	7.4	2326	1839	1674	1574	1507	65
	74	4.7	5.5	550	400	374	364	352	64
High-density polyethylene	223	1.4	3.3	4099	3881	3727	3629	3572	87
	148	3.2	4.3	1983	1896	1821	1774	1750	88
	74	3.0	3.5	598	542	514	503	495	83
Hydrous lactose	223	28.8	28.1	5707	1835	1598	1511	1490	26
	148	19.2	18.6	2386	966	852	809	793	33
	74	9.3	9.2	606	309	298	296	295	49
Klucel HXFNF	223	−1.4	−1.7	1903	1960	1933	1900	1885	99
	148	1.6	1.3	1106	1084	1062	1057	1048	95
	74	1.0	1.1	429	391	384	383	381	89
Klucel HXF	223	−0.8	−1.3	2180	2174	2119	2070	2034	93
	148	1.7	1.6	1186	1138	1105	1092	1079	91
	74	1.3	1.3	468	426	417	414	413	88
Myplx	223	3.0	4.2	3165	3086	3004	2966	2943	93
	148	5.2	6.2	1662	1592	1553	1531	1529	92
	74	4.0	5.3	626	559	539	530	515	82
Sodium chloride	223	84.0	80.6	12725	3361	3062	2918	2795	22
	148	50.6	50.6	5127	1127	1007	942	881	17
	74	17.8	18.6	984	248	226	209	190	19
Polyox 300K	223	−1.0	1.5	3687	3517	3457	3410	3385	92
	148	1.7	2.7	1829	1700	1654	1631	1615	88
	74	1.3	1.5	563	512	495	488	483	86
Polyox 7M	223	−1.0	1.5	3653	3539	3459	3419	3385	93
	148	1.7	2.7	1867	1760	1705	1674	1653	89
	74	1.3	1.5	552	496	485	479	476	86
PEG 1450	223	1.2	1.1	1500	1611	1623	1666	1700	113
	148	1.7	2.0	872	946	947	960	982	113
	74	1.9	2.0	390	377	373	370	370	95
PEG 8000	223	13.3	16.2	4174	3186	2923	2816	2759	66
	148	10.0	12.1	2253	1594	1447	1382	1346	60
	74	6.5	8.0	756	486	434	412	400	53
Sodium citrate	223	30.8	29.8	4974	1017	861	831	808	16
	148	20.7	19.4	2153	610	600	546	543	25
	74	9.2	9.3	527	227	208	198	192	36
Sucrose	223	31.7	35.1	6340	1829	1409	1213	1108	17
	148	25.0	26.4	3161	1042	886	800	743	24
	74	7.9	8.7	581	316	294	269	260	45

The percentage change is 100 ∗ hysteresis area cycle 5/hysteresis area cycle 1.

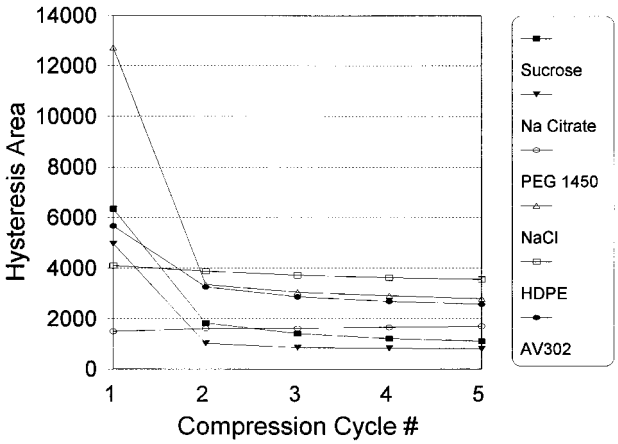

Figure 4. Hysteresis areas calculated as a function of the number of compression cycles.

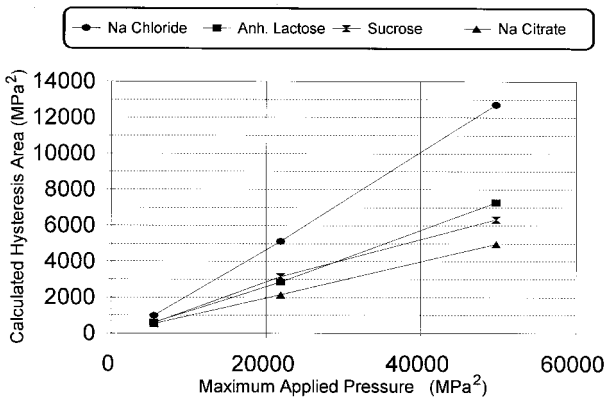

Figure 6. Hysteresis areas calculated for various brittle materials as a function of the square of maximally applied punch pressure.

where the hysteresis area is the sum of the area under the unloading profile minus the sum of the area under the loading profile, and p denotes the applied pressure over which the integration takes place. On integration, the hysteresis area is given by the following equation:

$$\textit{Hysteresis area} = 0.5\,(U - L)\,M^2 + LYM - 0.5\,UY^2 - 0.5\,LY^2 \quad (2)$$

If the unloading and loading slopes associated with the profile are equal to 1, which is a common assumption for plastic materials, then the equation becomes

$$\textit{Hysteresis area} = YM - Y^2 \quad (3)$$

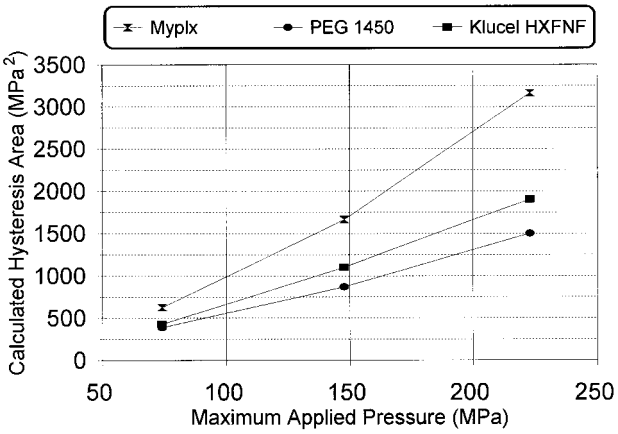

Figure 5. Hysteresis areas calculated for various plastic materials as a function of maximally applied punch pressure.

This equation indicates that the hysteresis area is related to the maximum peak pressure in a linear fashion.

Brittle Fracture Materials

For brittle fracture material, the model compression cycle profile for the first compression cycle is depicted in Fig. 8. In this figure, L denotes the loading slope, U denotes the unloading slope, M denotes the maximum applied punch pressure, R denotes the residual die wall, and F denotes the fracture point at which the relatively

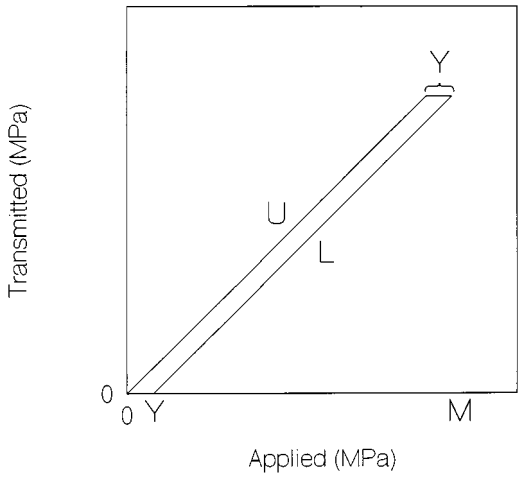

Figure 7. Simplified compression cycle profile for plastic materials used to derive a mathematical relationship between the calculated hysteresis areas and the maximally applied pressure.

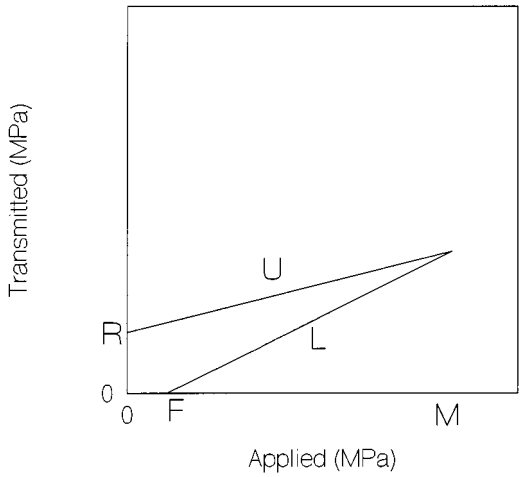

Figure 8. Simplified compression cycle profile for brittle fracture materials used to derive a mathematical relationship between the calculated hysteresis areas and the maximally applied pressure.

flat portion of the loading slope ceases and the loading slope describes the loading event. It is assumed that the quantity F is constant for brittle fracture materials. The hysteresis area for the brittle fracture compression cycle profile can then be calculated by the following equation:

$$\text{Hysteresis area} = \int_0^M (R + Up)dp - \int_F^M (Lp - LF)dp \quad (4)$$

where the hysteresis area is the sum of the area under the unloading profile minus the sum of the area under the loading profile. On integration, the hysteresis area is given by the following equation:

$$\text{Hysteresis area} = RM + 0.5\,UM^2 + 0.5\,LF^2 - 0.5\,LM^2 + LFM - LF^2 \quad (5)$$

where F is presumed to be constant. R can be expressed in terms of the following equation from the profile above $(M - F)L = UM + R$, yielding $R = (L - U)M - FL$. By substituting this into the above equation and solving it, the following equation is obtained:

$$\text{Hysteresis area} = 0.5\,(L - U)M^2 - 0.5\,LF^2 \quad (6)$$

In the case of brittle fracture material, the unloading and loading slopes are very different. Therefore, the hysteresis area is related to the square of the maximum pressure applied.

Classification of Materials Based on the Model Fits

The model equations derived above were used to fit the calculated hysteresis areas obtained as a function of applied pressure, which were presented in Table 1. In the case of the plastic model, the data were fitted for the value Y using nonlinear regression; in the case of the brittle model, the data were used to solve for the value F using the previously calculated loading and unloading slopes (3). The solved F values were then averaged and are reported in Table 2. The quality of the fits obtained for both the plastic model and the brittle fracture model was estimated by calculating the percentage deviation. The percentage deviation is defined as the average of (|fitted value − actual value|/actual value) ∗ 100 for each observation point. A lower value indicates a higher quality of fit to the actual data, whereas a higher number indicates that the quality of the fit to the actual data is not as good, which indicates that the model utilized is not appropriate for describing the behavior of the compound under study. The fitted values for the various compounds studied and the calculated percentage deviation values for both the plastic and brittle fracture models appear in Table 2. In comparing the plastic and the brittle fracture models in their ability to fit the data, the ratio of the percentage deviations calculated for the two models can be utilized to indicate readily which process or model is more accurate in describing the data. The P/B ratio is defined as the percentage deviation obtained for the plastic model divided by the percentage deviation obtained for the brittle fracture model for the compound of interest. A P/B ratio of less than 1 indicates that the plastic model is superior in fitting the data, whereas a value greater than 1 indicates that the brittle fracture model is superior in describing the data. The calculated P/B ratios are also reported in Table 2. The P/B ratios calculated were utilized to rank order the various compounds, and a plot of the compounds rank ordered using this parameter appears in Fig. 9.

The rank ordering obtained using the calculated P/B ratios for the first compression cycle are consistent with an earlier analysis (3), in which materials such as polyethylene glycol 8000, high-density polyethylene, polyox 7M, polyox 300K, Myplx, Klucel, and polyethylene glycol 1450 were classified to consolidate by plastic deformation, and materials such as sodium citrate, sucrose, an-

Table 2

Fitted Values and the Average Percentage Deviation Calculated Using the Model Plastic and Brittle Equations Developed

	First Compression Cycle					Fifth Compression Cycle				
	Plastic *Y*	% Deviation	Brittle *F*	% Deviation	P/B Ratio	Plastic *Y*	% Deviation	Brittle *F*	% Deviation	P/B Ratio
Acetaminophen	29.4	51.7	26.4	9.1	5.70	11.0	63.2	0	28.9	2.20
Anhydrous lactose	35.7	59.0	47.5	21.8	2.70	5.4	35.8	16.8	18.8	1.90
Aspirin	18.2	52.4	0	46.3	1.13	13.8	56.8	0	55.4	1.02
Avicel PH102	22.1	43.5	0	24.7	1.76	10.2	57.1	0	41.3	1.38
Avicel PH112	22.2	45.2	0	22.6	2.00	10.3	64.3	0	23.8	2.70
Avicel PH302	26.6	48.7	0	11.6	4.20	10.6	70.1	0	29.7	2.36
Cornstarch	22.7	47.4	0	90.0	0.53	14.4	60.9	0	86.2	0.71
High-density polyethylene	18.4	33.2	0	140	0.24	15.8	37.8	0	137	0.27
Hydrous lactose	26.3	50.1	23.5	7.5	6.68	6.4	22.4	0	33.3	0.67
Klucel HXFNF	8.5	13.6	0	194	0.07	8.3	19.5	0	196	0.10
Klucel HXF	9.6	16.8	0	177	0.09	8.8	20.2	0	188	0.11
Myplx	14.2	18.8	0	127	0.15	13.0	25.4	0	145	0.18
Sodium chloride	77.5	48.4	44.9	10.8	4.48	10.8	115	45.2	38	3.02
Polyox 300K	16.5	31.5	0	153	0.21	14.8	37.4	0	154	0.24
Polyox 7M	16.4	31.4	0	137	0.23	14.9	37.7	0	138	0.27
PEG 1450	6.7	8.9	0	224	0.04	7.5	15.7	0	211	0.07
PEG 8000	19.5	18.9	0	110	0.17	11.9	37.9	0	120	0.32
Sodium citrate	23.4	55.4	1.8	1.55	36.0	3.6	12.6	0	75.4	0.17
Sucrose	31.4	50.4	21.5	7.2	7.0	5.0	12.5	0	67	0.19

The average percent deviation indicates the goodness of fit to either model. The P/B ratio is the goodness of fit for the plastic model divided by the goodness of fit for the brittle model. A value less than 1 indicates that the plastic model is superior, and a value greater than 1 indicates that the brittle model is superior.

hydrous lactose, sodium chloride, hydrous lactose, and acetaminophen were classified to consolidate by brittle fracture. Furthermore, materials such as Avicel, cornstarch, and aspirin appeared to fall in between these two categories, which is consistent with the present observation.

The data for the fifth compression cycle are also analyzed and presented in Table 2. The model hysteresis cycle profiles for brittle fracture materials during subsequent compression cycles are expected to be representative of elastic deformation of the materials and as such would be very close in mathematical treatment to the plastic model derived above. Therefore, it is expected that the plastic model would describe the calculated hysteresis areas as a function of maximally applied pressure for both plastic materials and brittle fracture materials after the initial compaction of the material. For the most part, the calculated P/B ratios for the fifth compression cycle indicate agreement with this statement. However, there are a few exceptions to this, mainly the microcrystalline cellulose class of materials (various grades of Avicel). For classically brittle fracture materials such as sucrose and sodium citrate, the above statement is fully supported by the P/B ratios calculated.

Evaluation of Residual Die Wall Pressure as a Function of Maximum Applied Pressure

For brittle fracture materials, the model compression cycle profiles obtained indicate that the residual die wall pressure is related to the maximally applied punch pressure by the equation $R = (L - U)\,M - FL$, in which R represents the residual die wall pressure, L represents the loading slope, U represents the unloading slope, M represents the maximally applied punch pressure, and F represents the fracture point. A plot of the residual die wall pressures as a function of maximum applied pressure would then be linear, with the slope representing the difference in the loading and unloading slopes, and the intercept equaling the fracture pressure multiplied by the loading slope. Plots for sodium chloride, sucrose, and sodium citrate are presented in Fig. 10. The slope and the inter-

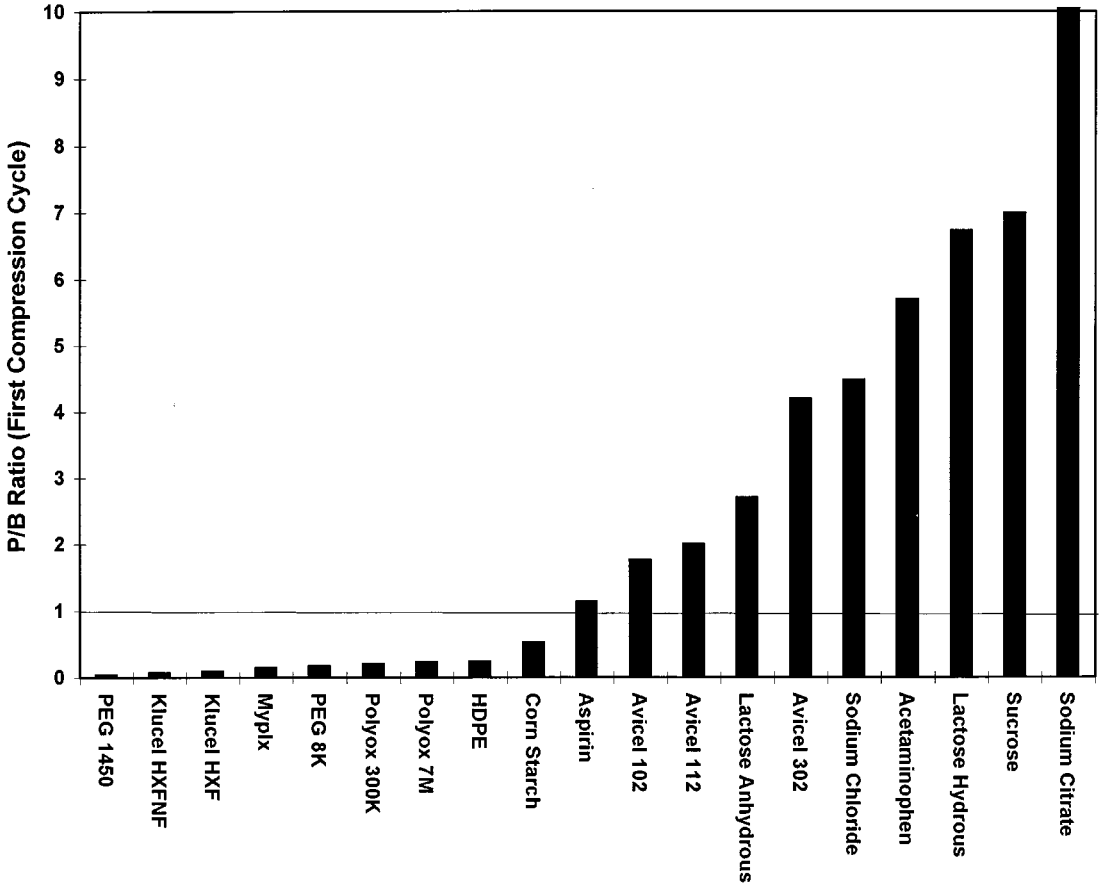

Figure 9. The calculated P/B ratios calculated for the various compounds studied. A P/B ratio of less than 1 indicates consolidation by a plastic mechanism, and a value greater than 1 indicates consolidation by brittle fracture.

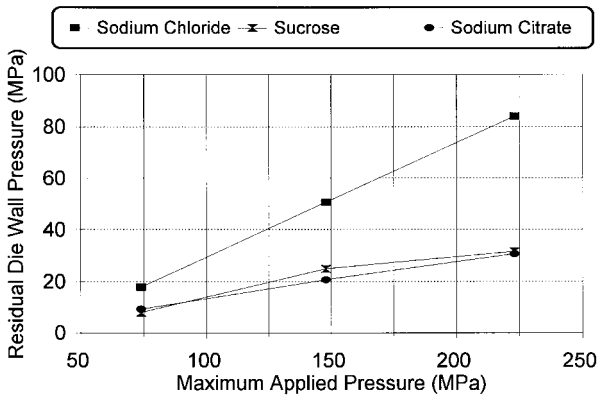

Figure 10. The residual die wall pressures as a function of maximum applied pressure for sodium chloride, sucrose, and sodium citrate.

cept of these lines were determined using linear least-squares regression. These values are presented in Table 3. For materials for which the calculated slopes are negative, there is an indication that the brittle fracture model utilized is not appropriate, which is consistent with the fact that these materials are known to consolidate by plastic deformation (3,5,7). For the brittle fracture materials, the calculated slopes based on the residual die wall pressures are in rough conformance with the differences in the loading and unloading slopes previously calculated based on the hysteresis cycle profiles.

CONCLUSIONS

1. The experimental data obtained indicate that a linear relationship exists between the hysteresis areas and maximally applied punch pressures for

Table 3

The Calculated Slope and Intercept Values for Plots of Residual Die Wall Pressures Versus the Maximim Applied Punch Pressure

	Slope	Intercept	Loading-Unloading Slope[a]
Acetaminophen	0.0550	3.1110	0.2624
Anhydrous lactose	0.1309	−0.3118	0.3317
Aspirin	0.0208	2.1092	0.0895
Avicel PH102	0.0140	7.1168	0.1533
Avicel PH112	0.0127	6.7158	0.1565
Avicel PH302	0.0388	6.1029	0.2003
Cornstarch	−0.0108	6.0670	0.0203
High-density polyethylene	−0.0108	4.1306	−0.0736
Hydrous lactose	0.1309	−0.3118	0.2391
Klucel HXFNF	−0.0141	2.8304	−0.0961
Klucel HXF	−0.0162	2.7972	−0.0867
Myplx	−0.0068	5.0697	−0.0429
Sodium chloride	0.4443	−15.1041	0.5527
Polyox 300K	−0.0155	2.9632	−0.0907
Polyox 7M	−0.0155	2.9632	−0.0629
PEG 1450	−0.0047	2.2975	−0.1039
PEG 8000	0.0456	3.1643	−0.0209
Sodium citrate	0.1449	−1.2666	0.1948
Sucrose	0.1596	−2.1366	0.2712

The slopes reported represent the loading minus the unloading slopes associated with the compression cycle profiles. The loading minus unloading slopes of the compression cycle profiles are calculated and reported for comparison purposes.

[a] These values were calculated using the previously reported loading and unloading slopes for compression cycle profiles (3).

plastic materials. For brittle fracture materials, the experimental data indicate that the hysteresis areas are related to the square of the maximally applied punch pressures.

2. Mathematical equations were derived for plastic and brittle fracture materials relating the calculated hysteresis areas and maximally applied punch pressures utilizing model compression cycle profiles. These relationships indicate that a linear relationship between hysteresis areas and maximally applied punch pressures exists for plastic materials, whereas for brittle materials, the hysteresis areas are related to the square of the maximally applied punch pressures.
3. The goodness of fit to the plastic and brittle fracture models derived was used to rank order the consolidation mechanism of the various compounds studied. This rank ordering is consistent with previous rank ordering, in which the unloading slopes associated with the compression cycle profiles were utilized.
4. Based on the goodness-of-fit data calculated, polyethylene glycol 1450 and Klucel are excellent model materials for plastically deforming materials, whereas sodium citrate and sucrose are excellent model materials for brittle fracture materials.
5. For brittle materials, the residual wall pressure is linearly related to the maximum applied punch pressure, whereas for plastic materials, the residual die wall pressure is negligible, and no relationship to the maximally applied punch pressure exists.

ACKNOWLEDGMENTS

Part of this work was presented by the author at the 30th annual Higuchi research meeting. The author wishes

to thank Dr. William Morehead and Dr. Richard Chang for extremely helpful discussions and suggestions.

REFERENCES

1. J. T. Carstensen and P. Toure, Compression cycles in tableting, Powder Technol., 26, 199–204 (1980).
2. J. T. Carstensen, J. P. Marty, F. Puisieux, and H. Fessi, Bonding mechanisms and hysteresis areas in compression cycle plots, J. Pharm. Sci., 2, 222–223 (1981).
3. D. Khossravi and W. T. Morehead, Consolidation mechanisms of pharmaceutical solids. A multi-compression cycle approach, Pharm. Res., 14, 1041–1047 (1997).
4. H. Leuenberger and W. Jetzer, The compactibility of powder systems—a novel approach, Powder Technol., 37, 209–218 (1984).
5. W. Jetzer, H. Leuenberger, and H. Sucker, The compressibility and compactibility of pharmaceutical powders, Pharm. Technol., 7, 33–39 (1983).
6. H. Leuenberger, The compressibility and compactibility of powder systems, Int. J. Pharm., 12, 41–47 (1982).
7. E. N. Hiestand and D. P. Smith, Indices of tableting performance, Powder Technol., 38, 45–59 (1984).
8. E. N. Hiestand and C. Peot, Tensile strength of compressed powders and an example of incompatibility as end-point on shear yield locus, J. Pharm. Sci., 63, 605–612 (1974).
9. S. T. David and L. L. Augsburger, Plastic flow during compression of directly compressible fillers and its effect on tablet strength, J. Pharm. Sci., 66, 155–159 (1977).
10. B. A. Obiorah, Possible prediction of compression characteristics from pressure cycle plots, Int. J. Pharm., 1, 249–256 (1978).
11. E. N. Hiestand and D. P. Smith, Tablet bond. II Experimental check of model, Int. J. Pharm., 67, 231–246 (1991).
12. W. M. Long, Radial pressures in powder compaction, Powder Metallurgy, 6, 73–86 (1960).
13. H. G. Cocolas and N. G. Lordi, Axial to radial pressure transmission of tablet excipients using a novel instrumented die, Drug Dev. Ind. Pharm., 19, 2473–2497 (1993).
14. E. G. Rippie and D. W. Danielson, Viscoelastic stress/strain behavior of pharmaceutical tablets: analysis during unloading and post compression periods, J. Pharm. Sci., 70, 476–482 (1981).